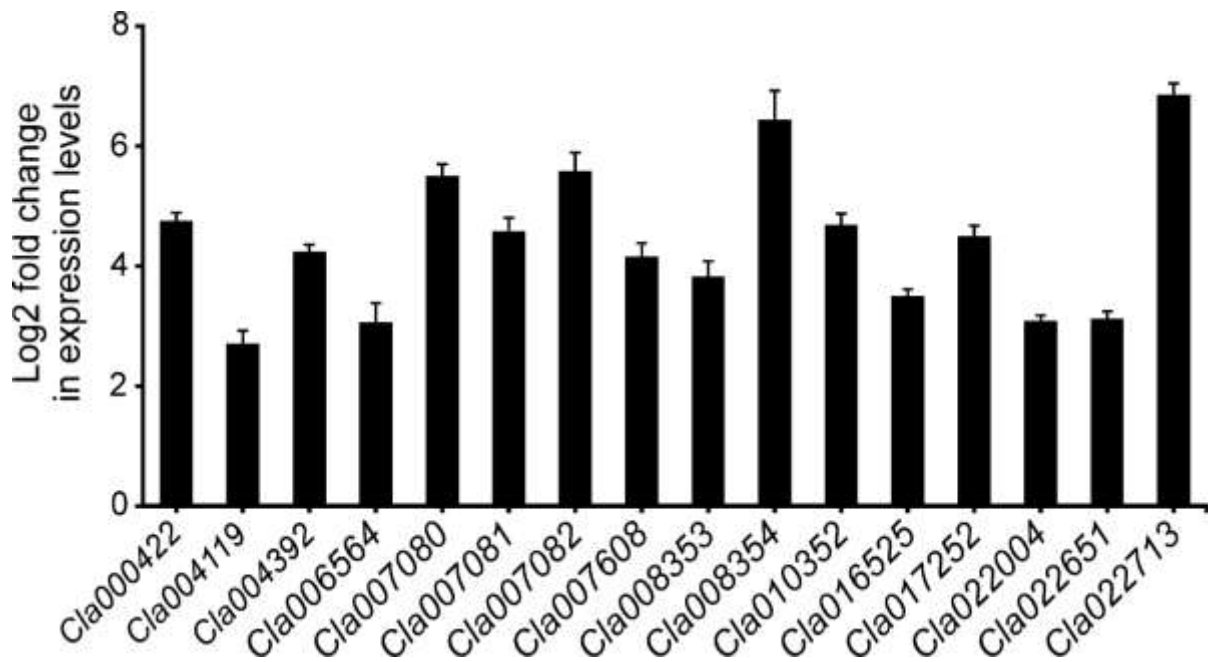
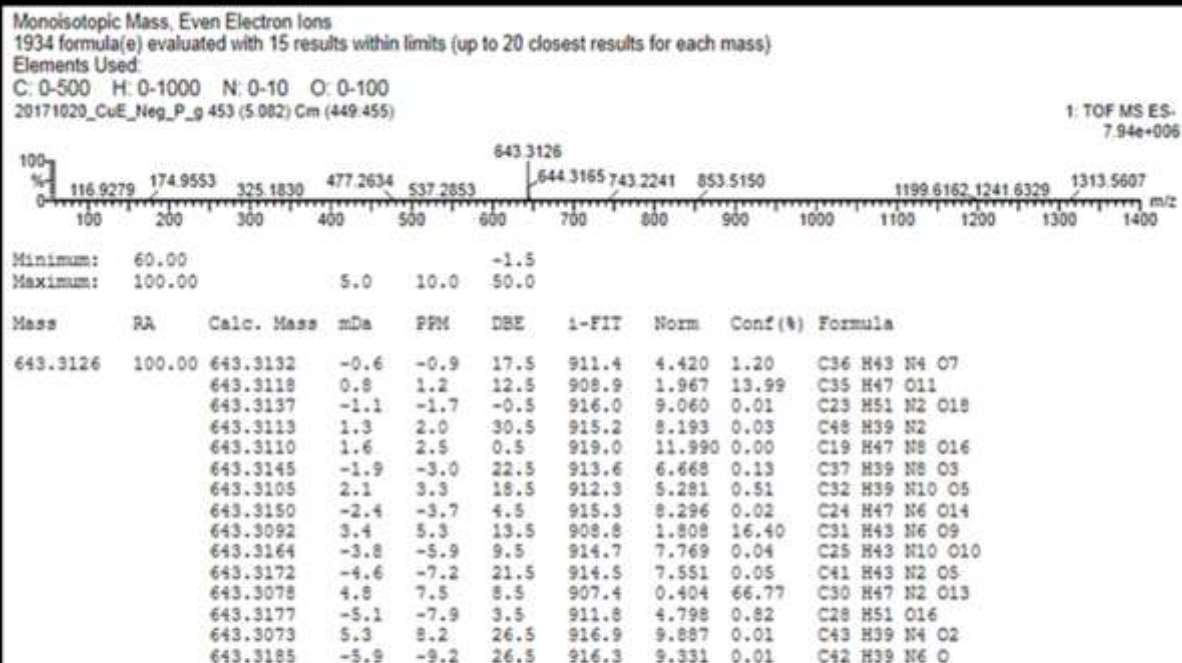


Supplementary information

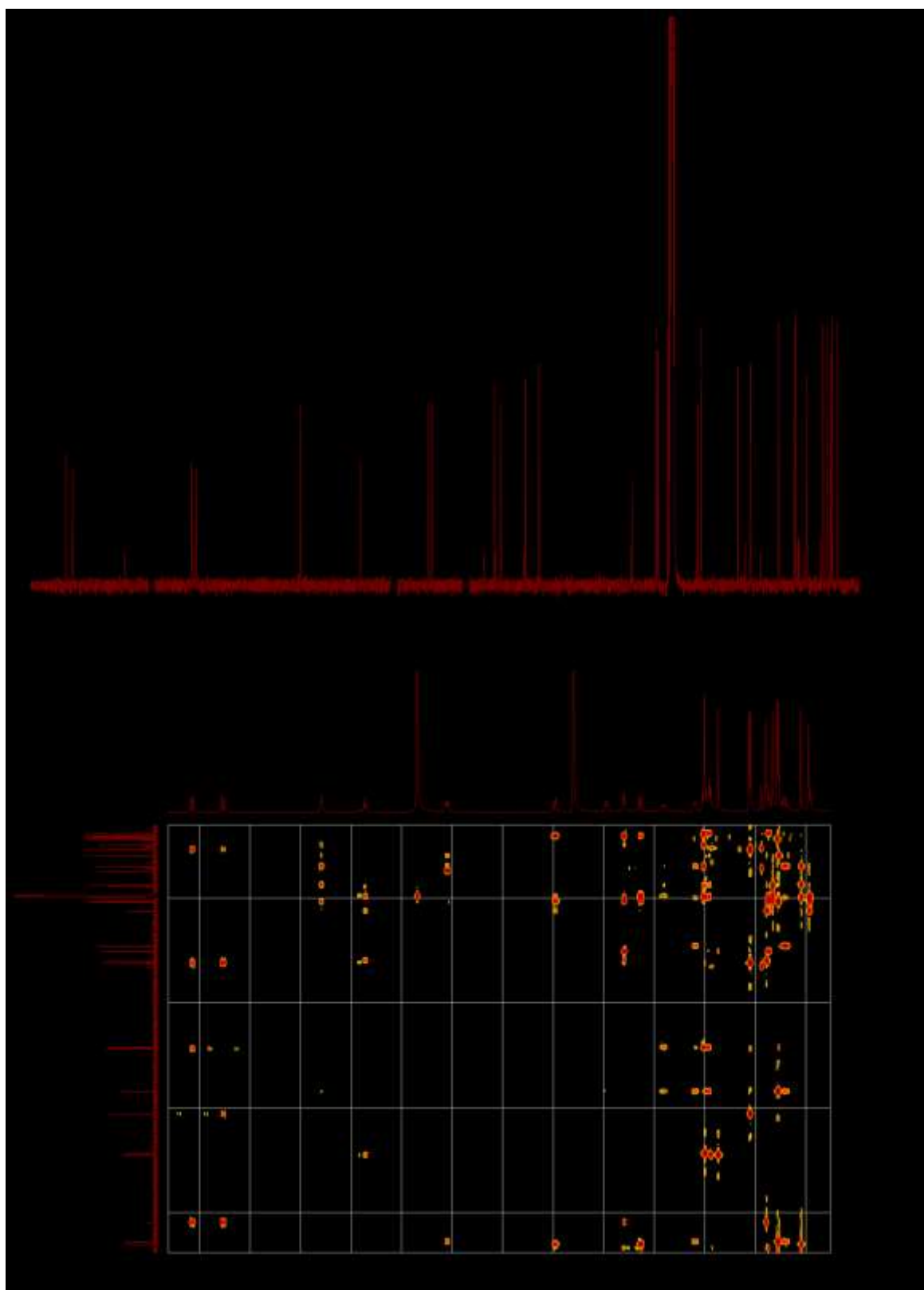
Supplementary Figures



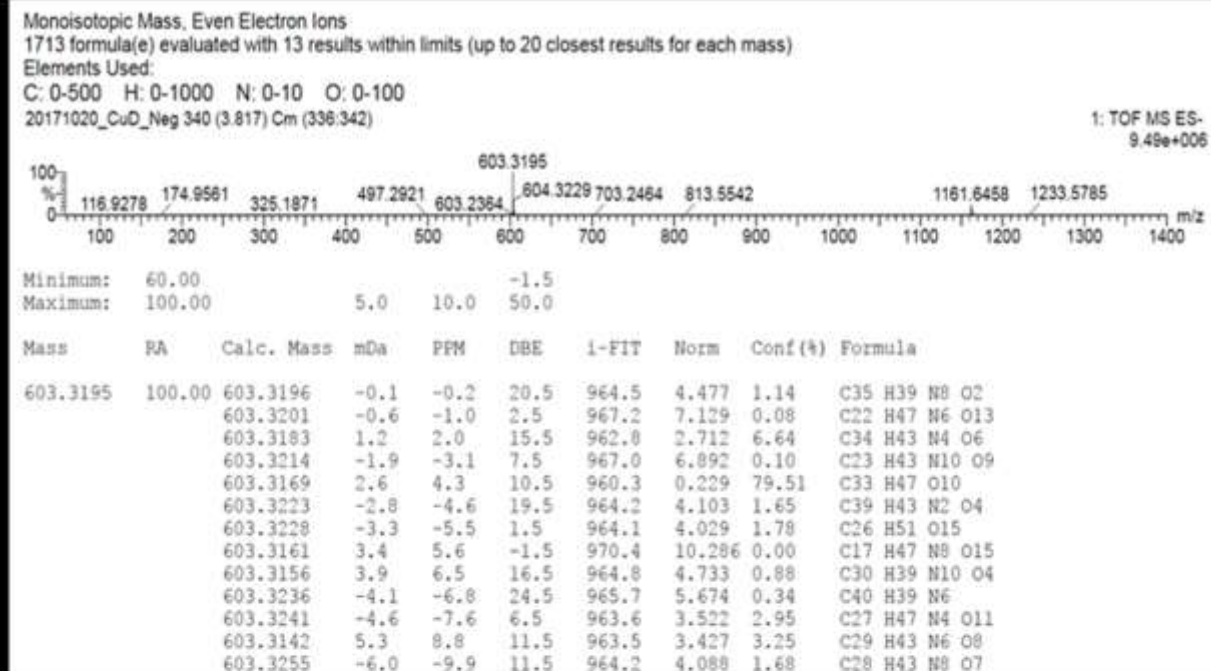
Supplementary Figure 1. RT-qPCR validation of up-regulated in PI532627 compare to PI536451. RT-qPCR analysis results showing log₂ fold change in expression for each gene expected to involve in cucurbitacins biosynthetic pathway.



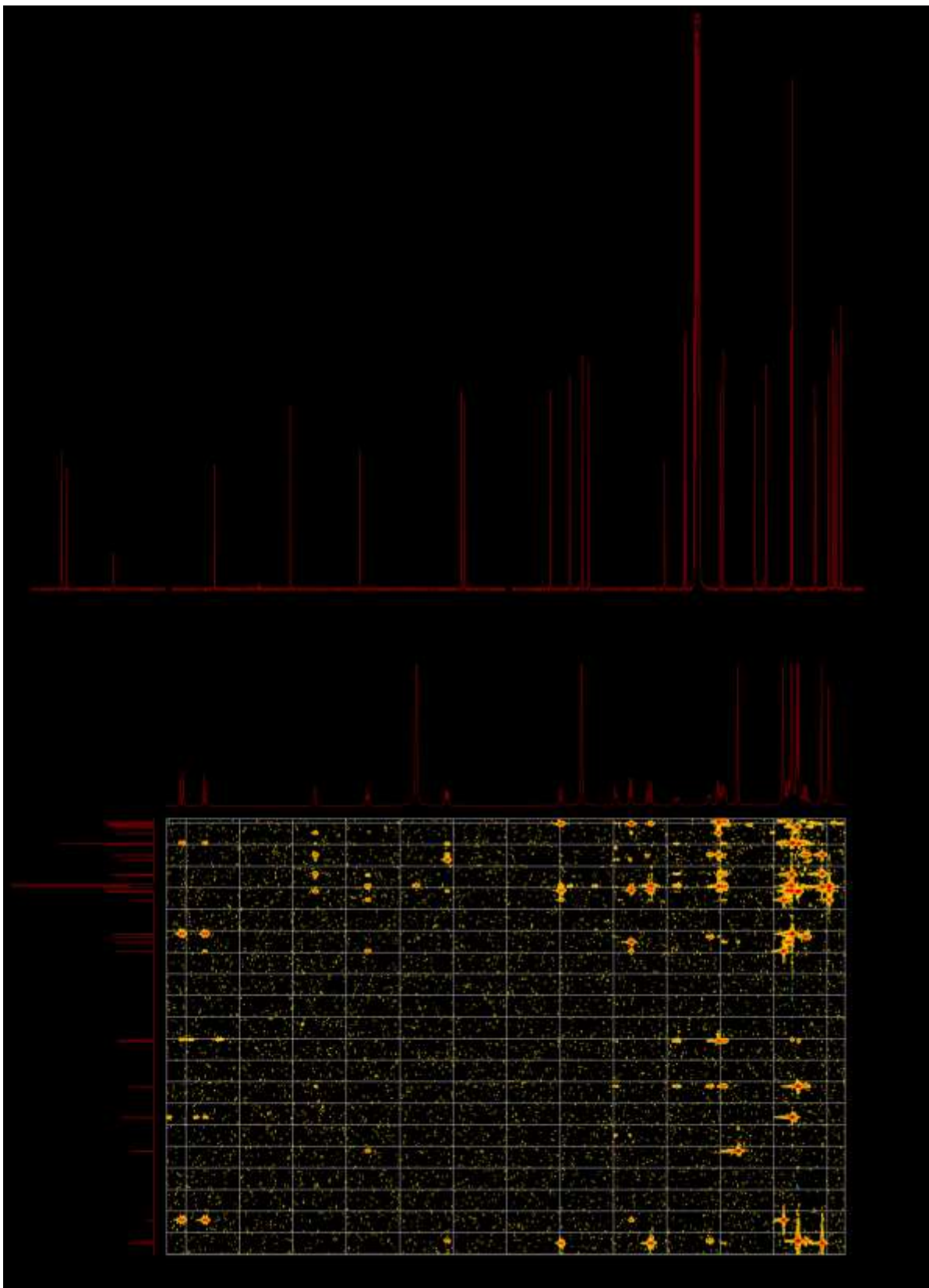
Supplementary Figure 2. HR-ESI/MS and $^1\text{H-NMR}$ results of compound 1 (16-*O*-acetyl cucurbitacin B). a, Negative HR ESI-MS m/z 645.3282 $[\text{M} + \text{formic acid-H}]^-$ (calculated for $\text{C}_{35}\text{H}_{49}\text{O}_{11}$ 645.3275) and (b) $^1\text{H-NMR}$ (600 MHz, CD_3OD , δ_{H}) in Table 2.



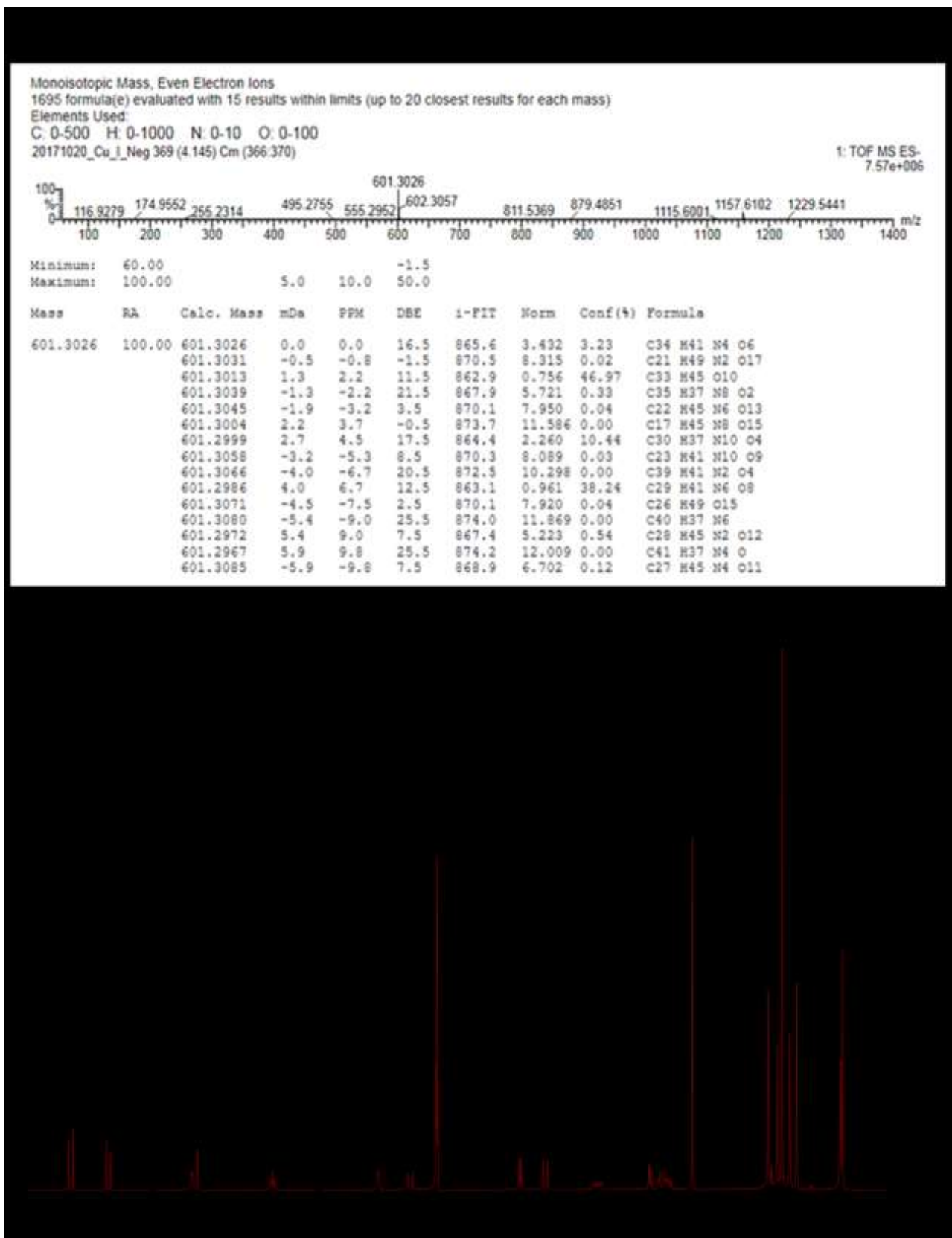
Supplementary Figure 3. ¹³C-NMR and HMBC results of compound 1 (16-*O*-acetyl cucurbitacin B). **a**, ¹³C-NMR (150 MHz, CD₃OD, δ_C) in Table 3 and **(b)** HMBC spectrum (CD₃OD, 600MHz).



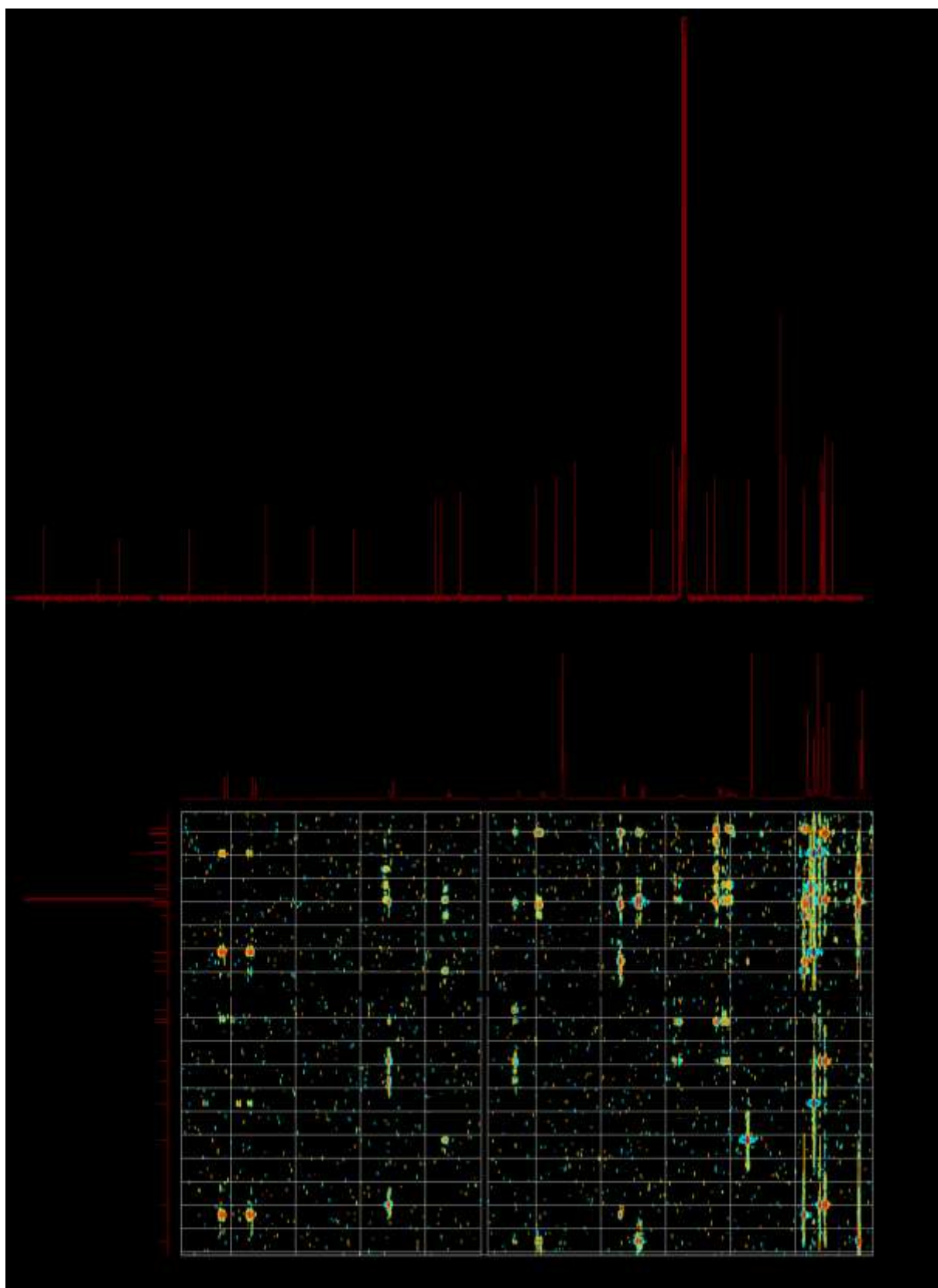
Supplementary Figure 4. HR-ESI/MS and ¹H-NMR results of compound 2 (16-*O*-acetyl cucurbitacin D). a, Negative HR ESI-MS m/z 603.3195 [$M+ \text{formic acid-H}$]⁻ (calculated for C₃₃H₄₇O₁₀ 603.3169) and (b) ¹H-NMR (600 MHz, CD₃OD, δ_H) in Table 2.



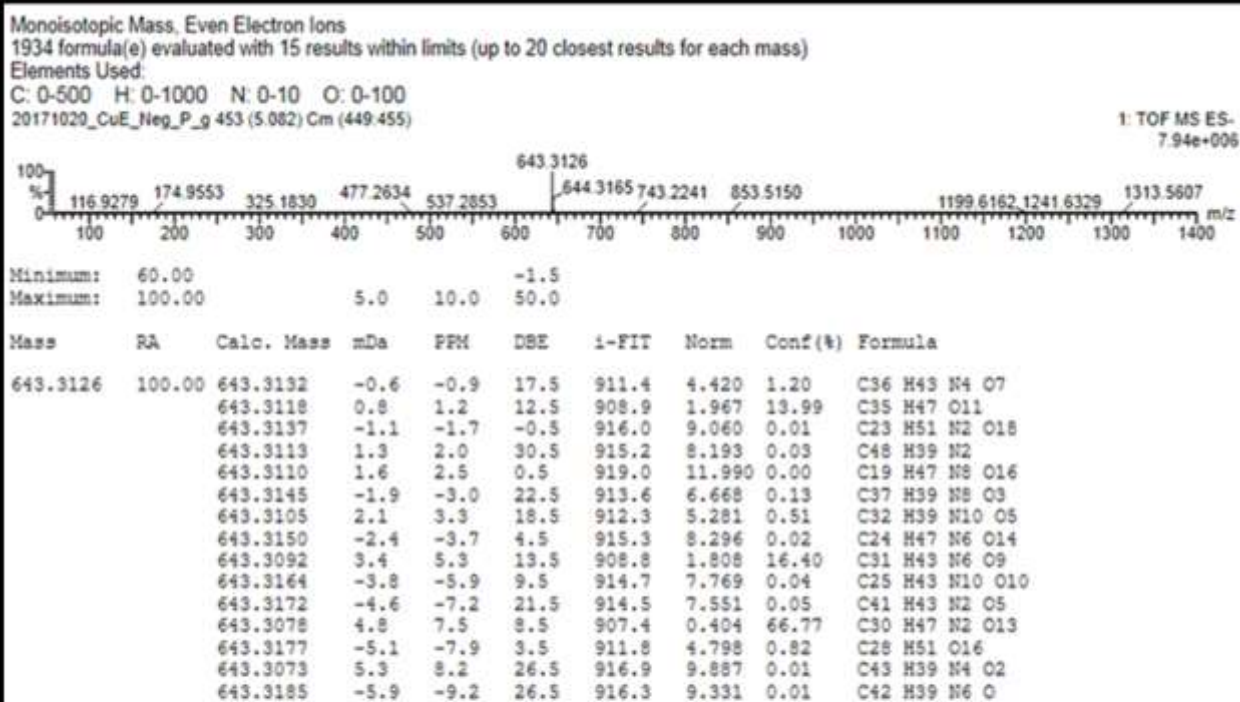
Supplementary Figure 5. ¹³C-NMR and HMBC results of compound 2 (16-*O*-acetyl cucurbitacin D). **a**, ¹³C-NMR (150 MHz, CD₃OD, δ_C) in Table 3 and **(b)** HMBC spectrum (CD₃OD, 600MHz).



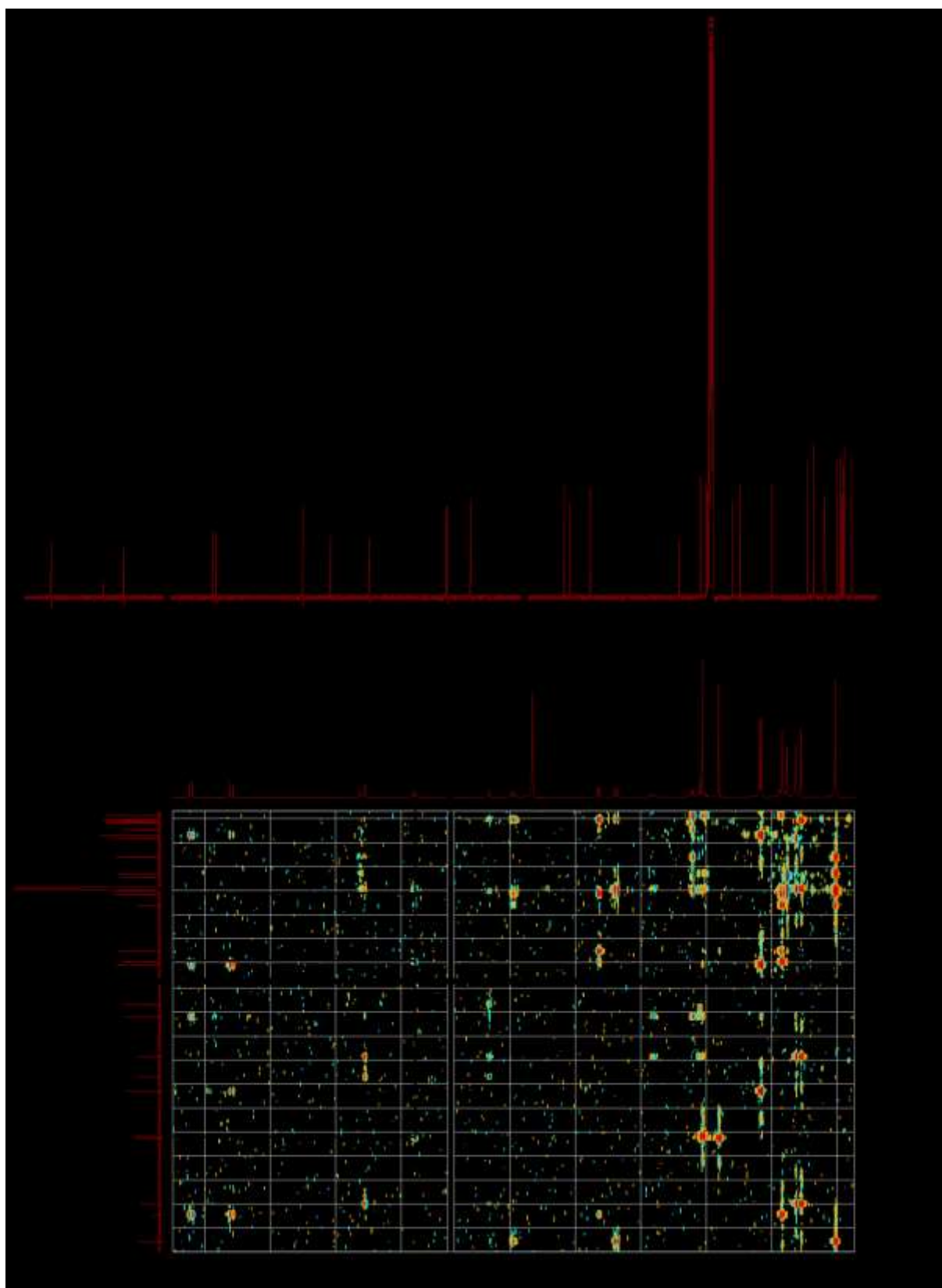
Supplementary Figure 6. HR-ESI/MS and ¹H-NMR results of compound 3 (16-*O*-acetyl cucurbitacin I). a, Negative HR ESI-MS m/z 601.3026 $[M + \text{formic acid-H}]^-$ (calculated for C₃₃H₄₅O₁₀ 601.3012) and (b) ¹H-NMR (600 MHz, CD₃OD, δ_H) in Table 2.



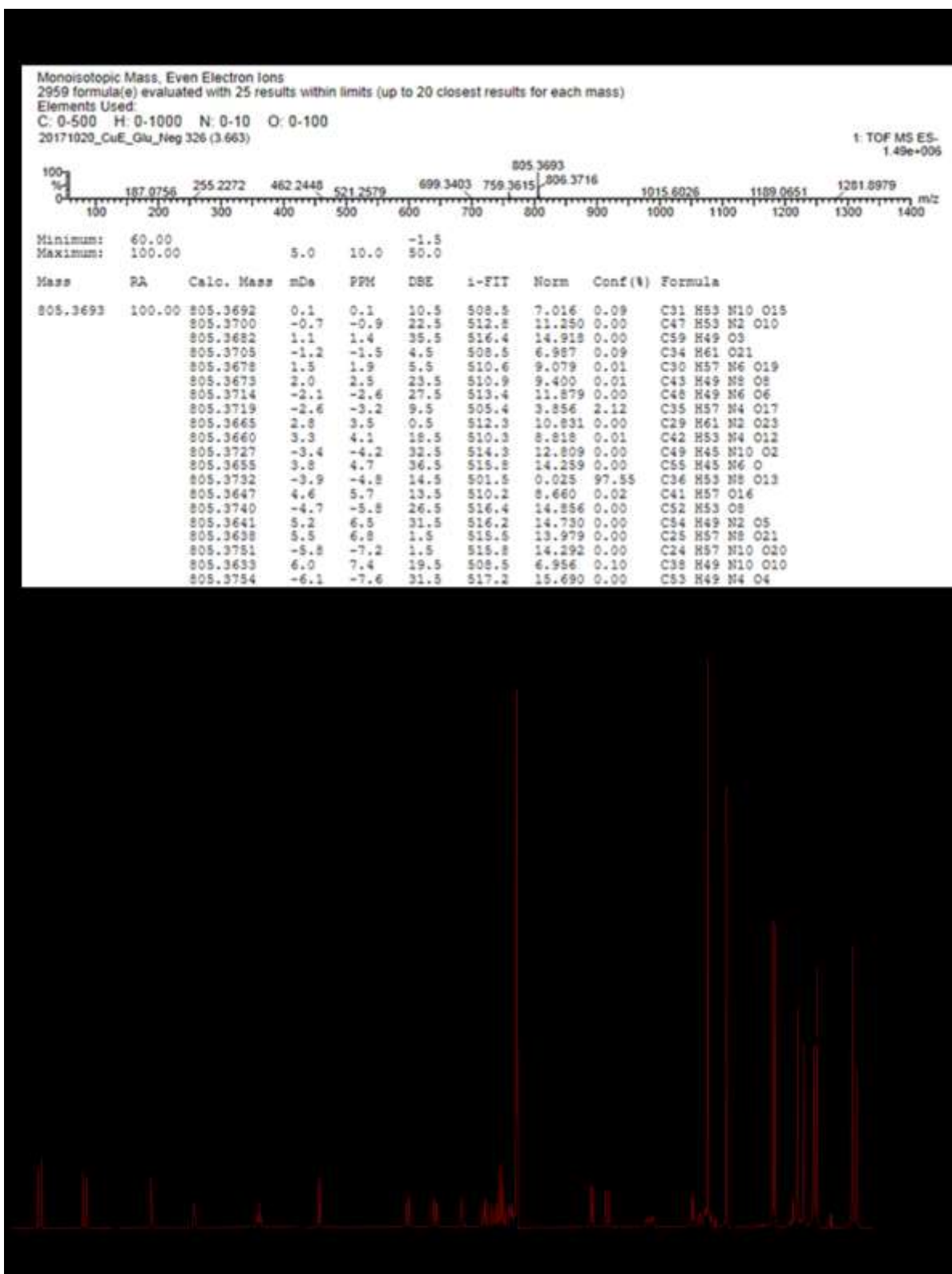
Supplementary Figure 7. ^{13}C -NMR and HMBC results of compound 3 (16-*O*-acetyl cucurbitacin I). **a**, ^{13}C -NMR (150 MHz, CD_3OD , δ_{C}) in Table 3 and **(b)** HMBC spectrum (CD_3OD , 600MHz).



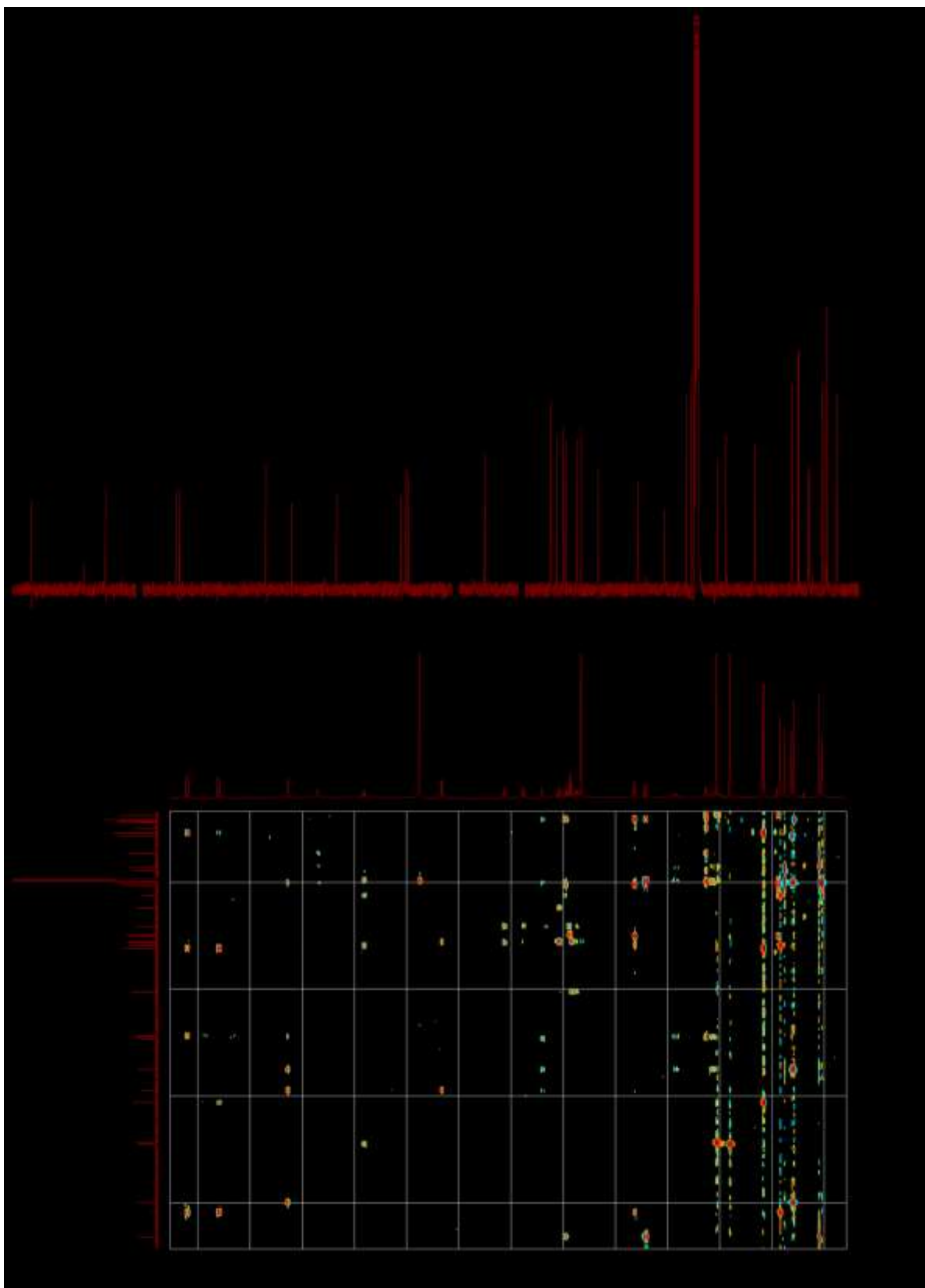
Supplementary Figure 8. HR-ESI/MS and $^1\text{H-NMR}$ results of compound 4 (16-*O*-acetyl curcurbitacin E). **a**, Negative HR ESI-MS m/z 643.3126 $[\text{M}^+ \text{formic acid-H}]^-$ (calculated for $\text{C}_{35}\text{H}_{47}\text{O}_{11}$ 643.3118) and **(b)** $^1\text{H-NMR}$ (600 MHz, CD_3OD , δ_{H}) in Table 2.



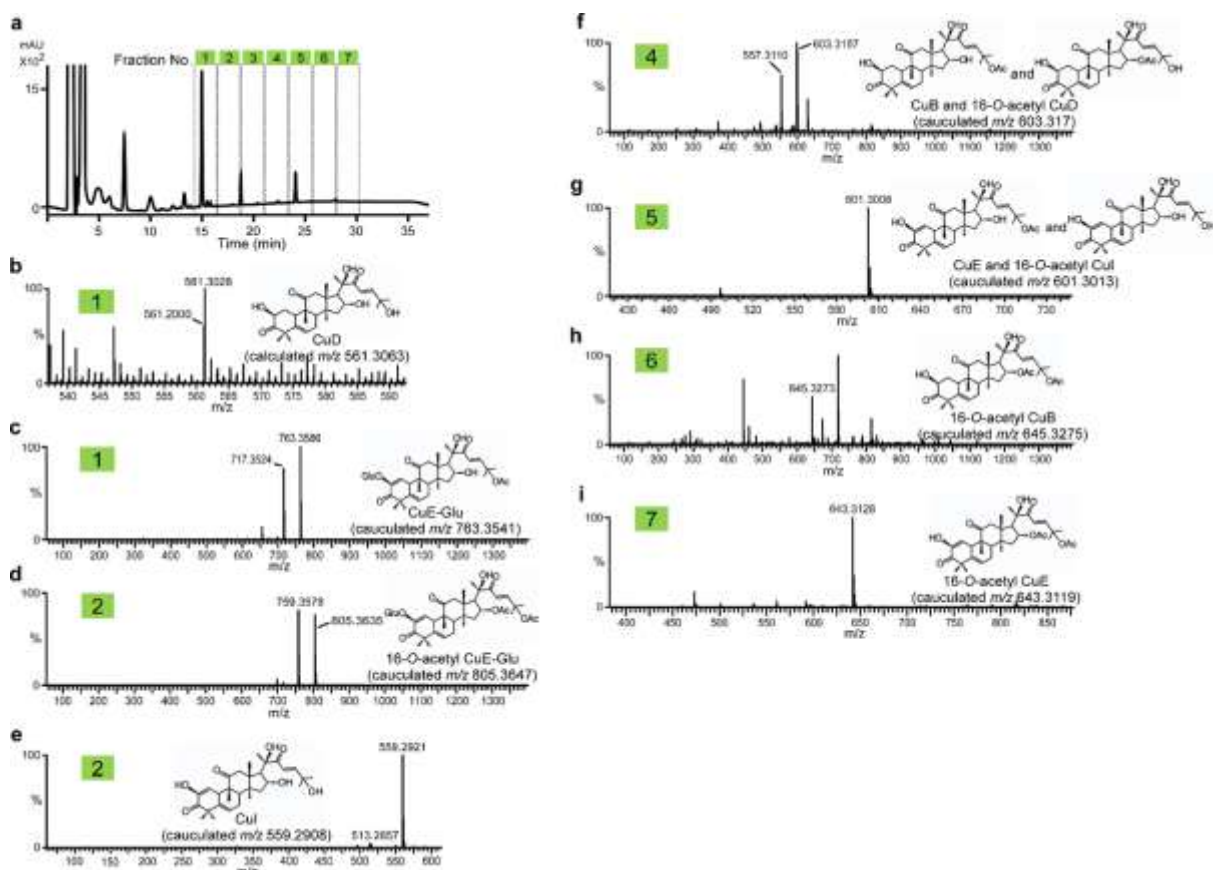
Supplementary Figure 9. ^{13}C -NMR and HMBC results of compound 4 (16-*O*-acetyl cucurbitacin E). **a**, ^{13}C -NMR (150 MHz, CD_3OD , δ_{C}) in Table 3 and **(b)** HMBC spectrum (CD_3OD , 600MHz).



Supplementary Figure 10. HR-ESI/MS and $^1\text{H-NMR}$ results of compound 5 (2-*O*- β -D-glucopyranosyl 16-*O*-acetyl cucurbitacin E). **a**, Negative HR ESI-MS m/z 805.3693 [$\text{M}+\text{formic acid-H}$] (calculated for $\text{C}_{41}\text{H}_{57}\text{O}_{16}$ 805.3646) and **(b)** $^1\text{H-NMR}$ (600 MHz, CD_3OD , δ_{H}) in Table 2.

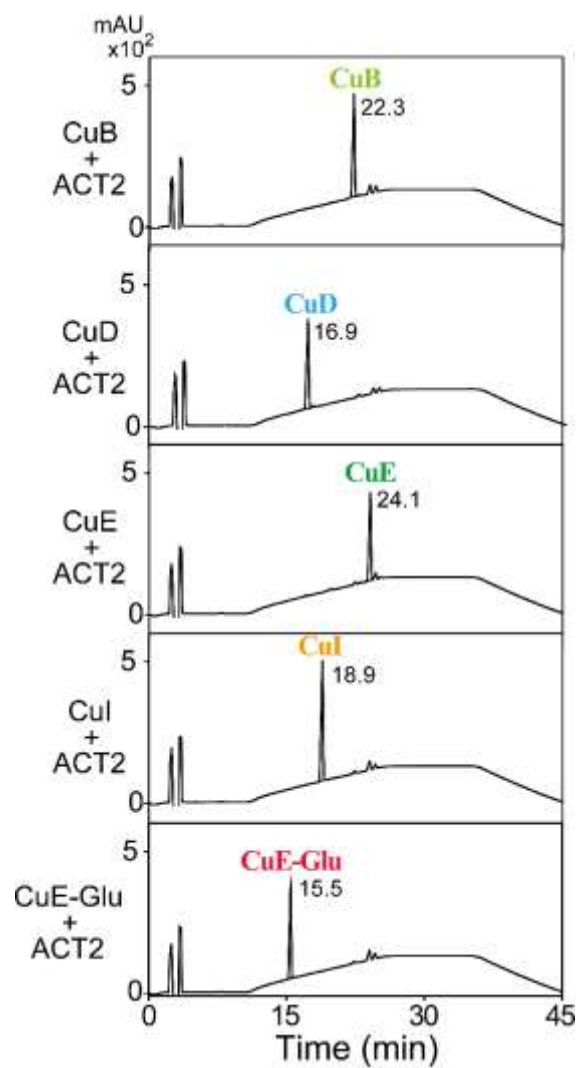


Supplementary Figure 11. ^{13}C -NMR and HMBC results of compound 5 (2-*O*- β -D-glucopyranosyl 16-*O*-acetyl cucurbitacin E). a, ^{13}C -NMR (150 MHz, CD_3OD , δ_{C}) in Table 3 and (b) HMBC spectrum (CD_3OD , 600MHz).

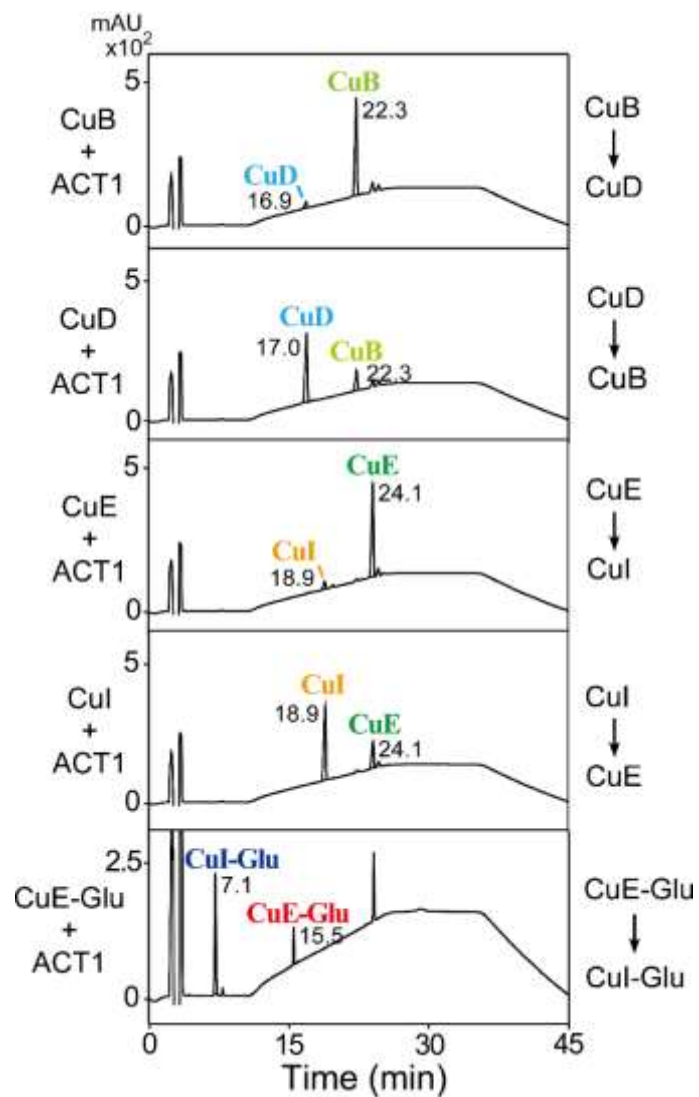


Supplementary Figure 12. Fractionation of watermelon extract during HPLC separation, and LC-MS analysis results of fractionated individual samples. a, HPLC chromatogram of watermelon extract for fractionations. **b**, LC-MS analysis of extract prepared from fraction number 1. The extracted ion chromatogram of the ion at m/z 561.3063 $[M+FA-H]^-$ corresponds to CuD. **c**, LC-MS analysis of extract prepared from fraction number 1. The extracted ion chromatogram of the ion at m/z 763.3541 $[M+FA-H]^-$ corresponds to CuE-Glu. **d**, LC-MS analysis of extract prepared from fraction number 2. The extracted ion chromatogram of the ion at m/z 805.3647 $[M+FA-H]^-$ corresponds to 16-*O*-acetyl CuE-Glu. **e**, LC-MS analysis of extract prepared from fraction number 2. The extracted ion chromatogram of the ion at m/z 559.2921 $[M+FA-H]^-$ corresponds to 16-*O*-acetyl CuI. **f**, LC-MS analysis of extract prepared from fraction number 4. The extracted ion chromatogram of the ion at m/z 603.3170 $[M+FA-H]^-$ corresponds to CuB and 16-*O*-acetyl CuD. **g**, LC-MS analysis of extract prepared from fraction number 5. The extracted ion chromatogram of the ion at m/z 601.3013 $[M+FA-H]^-$

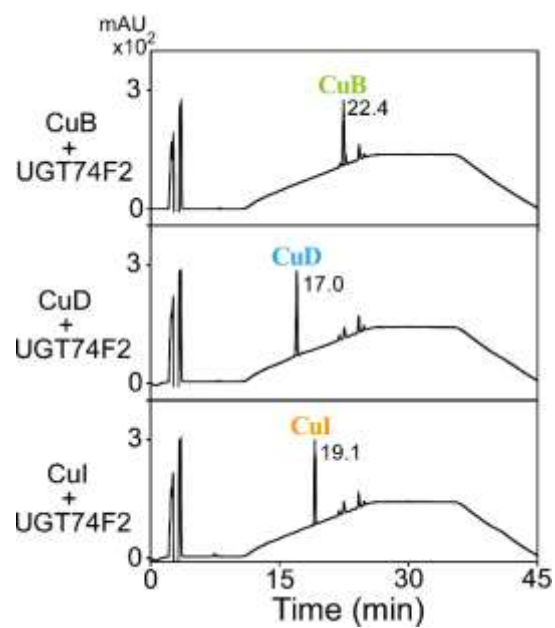
corresponds to CuE and 16-*O*-acetyl CuI. **h**, LC–MS analysis of extract prepared from fraction number 6. The extracted ion chromatogram of the ion at m/z 645.3275 $[M+FA-H]^-$ corresponds to 16-*O*-acetyl CuB. **i**, LC–MS analysis of extract prepared from fraction number 7. The extracted ion chromatogram of the ion at m/z 643.3119 $[M+FA-H]^-$ corresponds to 16-*O*-acetyl CuE. Round brackets indicate calculated m/z .



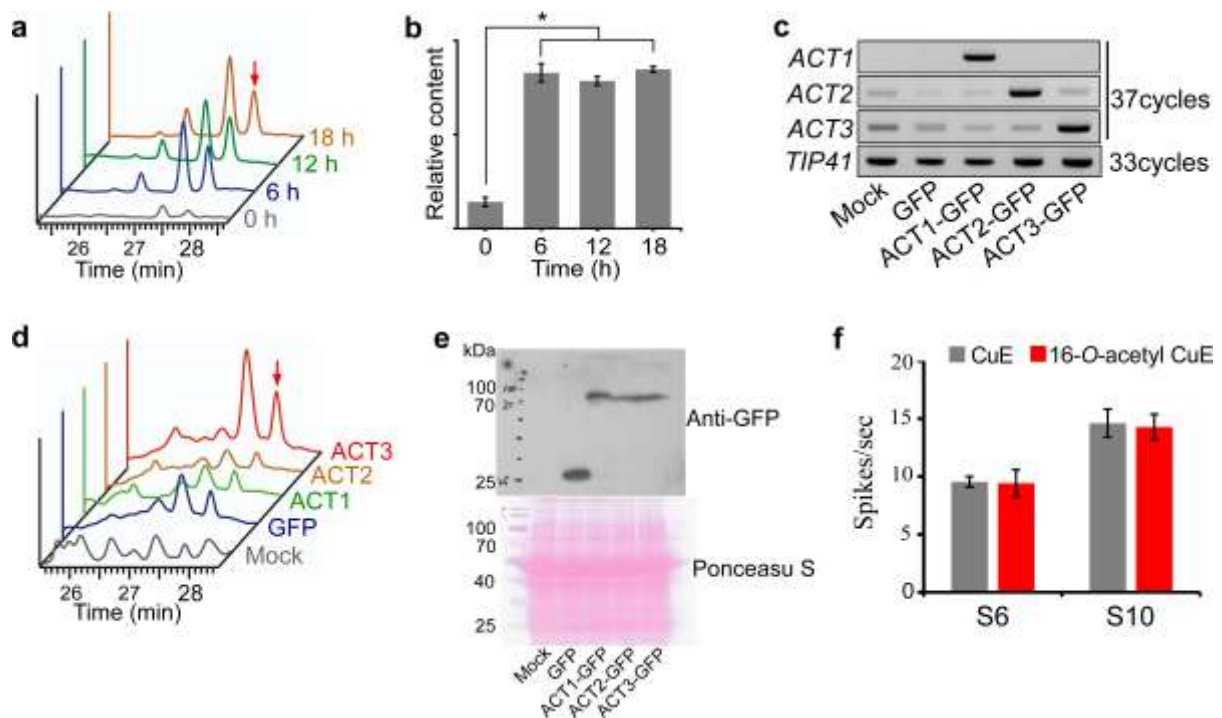
Supplementary Figure 13. ACT2 catalytic activity. HPLC analysis of ACT2 *in vitro* enzymatic reaction in the presence of the CuB, CuD, CuE, CuI and CuE-Glu which were used as a substrate.



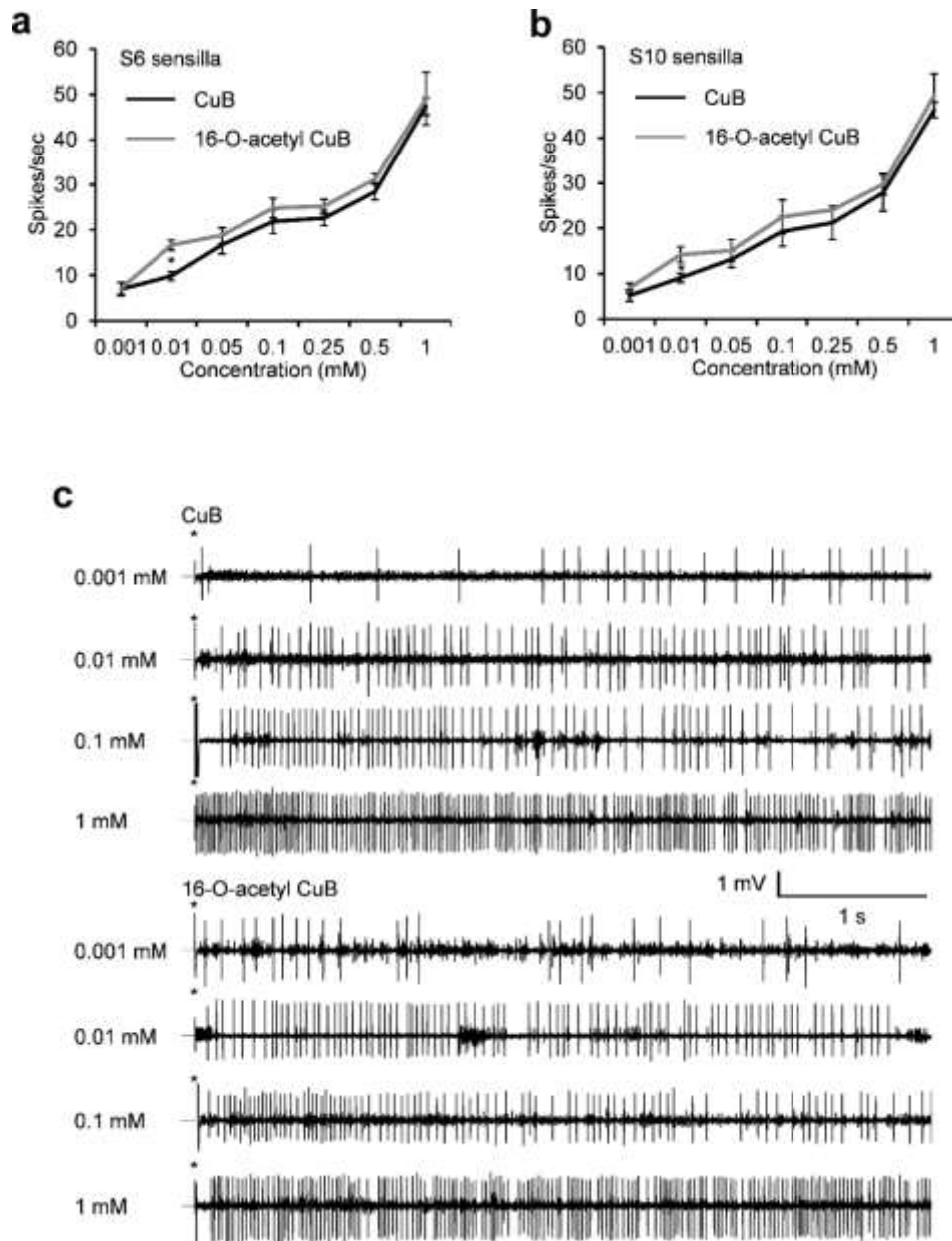
Supplementary Figure 14. ACT1 catalytic activity. HPLC analysis of ACT1 *in vitro* enzymatic reaction in the presence of the CuB, CuD, CuE, CuI and CuE-Glu which were used as a substrate.



Supplementary Figure 15. UGT74F2 catalytic activity. HPLC analysis of UGT74F2 *in vitro* enzymatic reaction in the presence of the CuB, CuD and CuI which were used as a substrate.



Supplementary Figure 16. Cucurbitacins accumulated by injury and *ACT3* transiently over expression, and evaluation of neuronal activation against *Drosophila*. **a**, HPLC chromatogram of 16-*O*-acetyl CuE in wounded leaves. **b**, Accumulation pattern of 16-*O*-acetyl CuE in wounded leaves were estimated by HPLC analysis. **c**, Semi RT-qPCR analysis results of leaves transiently overexpressed *ACTs* genes. **d**, HPLC chromatogram of 16-*O*-acetyl CuE in leaves transiently over expressed *ACT3* gene. **e**, Full immunoblot image of transiently overexpression *ACT* genes. **f**, The neuronal activation with CuE and 16-*O*-acetyl CuE. Average frequencies of action potential elicited from S6 and S10 sensilla (n=18-22). Red arrows indicate peaks of 16-*O*-acetyl CuE. The error bars represent \pm SD (n = 3). Asterisks indicate significant difference (*, $P < 0.05$)



Supplementary Figure 17. The dose-dependent neuronal with CuB and 16-O-acetyl CuB.

a, Average frequency of action potentials induced by the indicated concentrations of CuB and 16-O-acetyl CuB on S6 sensilla (n = 16-22). **b**, Average frequency of action potentials induced by the indicated concentrations of CuB and 16-O-acetyl CuB on S10 sensilla (n = 16-22). **c**, Representative sample traces obtained from S6 in **a**. All error bars represent SEMs. Single factor ANOVA with Scheffé's analysis was used as a post hoc test to compare two sets of data. Asterisks indicate statistical significance compared with each genotype (*, $P < 0.05$).

Supplementary Tables

Supplementary Table 1. Summary statistics of sequencing data collected from seedling transcriptomes.

USDA ID	Total reads	Filtered reads	Filtered reads (%)	Reads mapped	Reads mapped (%)
PI532627	54,301,266	53,379,720	93.0	47,619,535	85.63
PI536451	52,981,816	51,980,816	92.6	46,892,579	85.50

Total reads: sequences of obtained sequencing process. Filtered reads: low quality reads filtered according to the criteria. Read mapped: map reads to genome.

Supplemental Table 2. Descriptions and changes of the up-regulated genes in PI532627 compare to PI536451 seedling.

Gene ID	Gene name	Description	Log2FC
<i>Cla000422</i>	<i>UGT74E2</i>	UDP-glycosyltransferase 74E2	3.22
<i>Cla004119</i>	<i>GLYT3</i>	Probable glycosyltransferase	1.13
<i>Cla004392</i>	<i>UGT74F2</i>	UDP-glycosyltransferase 74F2	3.23
<i>Cla006564</i>	<i>UGT76F1</i>	UDP-glycosyltransferase 76F1	2.48
<i>Cla007080</i>	<i>CPQ</i>	Cucurbitadienol synthase	4.65
<i>Cla007081</i>	<i>BAHD1^a</i>	BAHD acyltransferase	3.55
<i>Cla007082</i>	<i>CYP87A3^b</i>	Cytochrome P450 87A3	3.83
<i>Cla007608</i>	<i>crtN</i>	Dehydrosqualene desaturase	3.15
<i>Cla008353</i>	<i>BAHD1^a</i>	BAHD acyltransferase	3.14
<i>Cla008354</i>	<i>CYP87A3^b</i>	Cytochrome P450 87A3	4.74
<i>Cla010352</i>	<i>UGT90A1</i>	UDP-glycosyltransferase 90A1	4.09
<i>Cla016525</i>	<i>UGT83A1</i>	UDP-glycosyltransferase 83A1	1.60
<i>Cla017252</i>	<i>CYP705A5</i>	Cytochrome P450 705A5	3.25
<i>Cla022004</i>	<i>UGT74E2</i>	UDP-glycosyltransferase 74E2	2.32
<i>Cla022651</i>	<i>SE</i>	Squalene monooxygenase	2.48
<i>Cla022713</i>	<i>ACT</i>	Vinorine synthase	Inf.

“Inf.” represent infinity. Log2FC: log2 fold change. *a*: genes described as same *CYP87A3*

gene name. *b*: genes described as same *BAHD1* gene name.

Supplementary Table 3. Primer sequences used in this study.

Gene	Purpose	Sequence (5' to 3')	Direction
<i>Cla000422</i>	RT-qPCR	ACAGCTGAGAAAGGGTTGGT	F
		GCACTCCCAAACCTCAATGCT	R
<i>Cla004119</i>	RT-qPCR	TGCATCTGTCCAAAGGGCTA	F
		GCTTCCCATTCCAACACCTC	R
<i>Cla006564</i>	RT-qPCR	ATGGTGGGTGAACGAGGATT	F
		ATCGGAACCCCTTCGCATAT	R
<i>Cla007080</i>	RT-qPCR	CATCCAGGCCATAGGACCAA	F
		CCCTTTATGCCAAACCACCC	R
<i>Cla007082</i>	RT-qPCR	GCTCTCCGCGACATTGAAAA	F
		CCGATGGATTCTCTGCAAGC	R
<i>Cla007608</i>	RT-qPCR	GTGGAGGTTGTGGTTTTTCGA	F
		TGAAGACCATGAATCCGAGGT	R
<i>Cla008354</i>	RT-qPCR	GCCAGGCACAACCTACAACA	F
		TCATTGCCCGTTCCTTTAGC	R
<i>Cla010352</i>	RT-qPCR	TACAGCGATTTGGACCCAGT	F
		CGATCAATCCGTAGCTGCTG	R
<i>Cla016525</i>	RT-qPCR	CGTGGGAAGATTGTGGGTTG	F
		GTACGGCCAACACAGGAATC	R
<i>Cla017252</i>	RT-qPCR	GCGGTAGTGAAGGAGTGTCT	F
		GATCCACTGCAACCATGGTG	R
<i>Cla022004</i>	RT-qPCR	AGGGTGAAGCTGGATGAACA	F
		CCACCTTCATCCATGGCTTC	R
<i>Cla022651</i>	RT-qPCR	GGCATCTGGATTGGAGCAAG	F
		CCGTTGCTGGGAAGAACATC	R
<i>ACT1</i> (<i>Cla007081</i>)	RT-qPCR	GCTTCCAAAATCGCTTCCCT	F
		GAAATCCCGGACGTTGCTTT	R
	Semi RT-qPCR	GCTTCCAAAATCGCTTCCCT	F
		GAAATCCCGGACGTTGCTTT	R
	Recombinant protein	caaatgggtcgcgatccATGGAGTCAGCATTG	F
		AAA	
	Transient expression	gtggtggtggtgctcgagGTGTTGGAGCTGAAG	R
		AAC	
	Transient expression	aacacgggggactctagaATGGAGTCAGCATTG	F
		AAAG	
Transient expression	ttatatctccttgatccTGTGTTGGAGCTGAAGA	R	
	ACA		
<i>ACT2</i> (<i>Cla008353</i>)	RT-qPCR	TAGTAGTTGGAGCCGGTTCG	F
		GTGTCCGTTAGCACCACAAA	R
Semi RT-qPCR	Semi RT-qPCR	GCCAGGCACAACCTACAACA	F
		TCATTGCCCGTTCCTTTAGC	R

	Recombinant protein	caaatgggtcgcggatccATGGAAGTTCAAATT CTC gtggtggtggtgctcgagGGAAAGGACACTAGG GTT	F R
	Transient expression	aacacgggggactctagaATGGAAGTTCAAATT CTCA ttatatccttgatccTGGAAAGGACACTAGG GTTT	F R
	RT-qPCR	GTTACTGTGGCGGCGTTTAA TGATTGTGTTGGAAGGCAGC	F R
	Semi RT-qPCR	GTTACTGTGGCGGCGTTTAA TGATTGTGTTGGAAGGCAGC	F R
<i>ACT3</i> (<i>Cla022713</i>)	Recombinant protein	caaatgggtcgcggatccATGGGGACGATGAAT TAC gtggtggtggtgctcgagATTGGCACTTGGGTTC AA	F R
	Transient expression	aacacgggggactctagaATGGGGACGATGAAT TACA ttatatccttgatccTATTGGCACTTGGGTTC AAA	F R
	RT-qPCR	AGTGAAGGTGGGTGAGGATG CTGCCACCTTTCCTAAGTGC	F R
<i>UGT74F2</i> (<i>Cla004392</i>)	Recombinant protein	caaatgggtcgcggatccATGGGTTTAGAAGGG AAA gtggtggtggtgctcgagAACACTTGGTATCTTG TC	F R
<i>TIP41</i> (<i>Cla016074</i>)	RT-qPCR	GCTCATGAGACTGAGGGACA CGAGAGCTTGAAACGTAGCC	F R
	Semi-qPCR	GCCTTTGATGCTCTGACTGG CGAGAGCTTGAAACGTAGCC	F R

Lower case indicate the plasmid DNA sequences.

Supplementary Methods

Plant material for RNA sequencing

Two *Citrullus lanatus* germplasms were used in this study. The seeds of PI532627 (USDA plant ID) and PI536451 (USDA plant ID) were kindly provided by the United States Department of Agriculture Germplasm Resources Information Network (USDA GRIN). Watermelon plants were grown in a growth chamber at 28°C under long-day conditions (photoperiod, 16 h : 8 h, light : dark) at a light intensity of 120 $\mu\text{mol m}^{-2} \text{s}^{-1}$. Seedlings were harvested 13 days after germination for RNA sequencing and RT-qPCR analysis.

Construction of RNA sequencing libraries

Libraries were prepared for 100 bp paired-end sequencing using the TruSeq RNA Sample Preparation Kit (Illumina). Specifically, mRNA was purified and fragmented from 2 μg of total RNA using oligo (dT) magnetic beads. The fragmented mRNAs were synthesized as single-stranded cDNAs through random hexamer priming. Double-stranded cDNA was prepared using single-stranded cDNA as a template for second-strand synthesis. After sequential end repair processes, A-tailing, and adapter ligation, cDNA libraries were amplified via polymerase chain reaction (PCR). The quality of these cDNA libraries was evaluated using the Agilent 2100 BioAnalyzer (Agilent) and quantified using the KAPA library quantification kit (Kapa Biosystems), according to the manufacturer's instructions.

RNA sequencing and transcriptome analysis

Paired-end sequencing (2×100 bp) was performed using Illumina HiSeq2500 (Illumina). Low-quality reads were filtered according to the following criteria; reads containing more than 10% skipped bases (marked as 'N's); reads containing more than 40% of bases with quality scores < 20 ; and reads where the average quality score for each read is < 20 . The filtering process was

performed using in-house scripts. Filtered reads were mapped to the reference genome related to the species using the aligner¹. Gene expression was measured with Cufflinks v2.1.1² using the gene annotation database for the species. Non-coding gene regions were excluded from the analysis of gene expression using the `-mask` option. To improve the accuracy of the measurement, multi-read-correction and frag-bias-correct options were applied. Default settings were used for all other options. Differential expression analysis was performed by Cuffdiff³. To enhance accuracy, multi-read-correction and frag-bias-correct options were applied. Default settings were used for all other options. DEGs were identified based on a q-value threshold less than 0.05 for correcting errors caused by multiple-testing⁴. The GO database classifies genes according to the three categories: Biological Process (BP), Cellular Component (CC), and Molecular Function (MF), and provides information on the function of genes. To characterize the genes identified from DEG analysis, a GO-based trend test was performed through the Fisher's exact test⁵. Selected genes with P-values < 0.001 following the test were regarded as statistically significant.

Elucidation of compound 1 (16-*O*-acetyl cucurbitacin B) structure by MS and NMR spectroscopy data analysis

The molecular formula of compound 1 was determined to be C₃₄H₄₈O₉ based on the negative ESI-MS *m/z* 645 [M+formic acid-H]⁻ and high resolution ESI-MS *m/z* 645.3282 [M+formic acid-H]⁻ (calculated for C₃₅H₄₉O₁₁ 645.3275) (Supplementary Fig. 2a). The ¹H-NMR spectrum (600 MHz, CD₃OD, δ_H) presented proton signals due to eight singlet methyls [δ_H 1.56 (H-27), δ_H 1.54 (H-26), δ_H 1.39 (H-30), δ_H 1.33 (H-29), δ_H 1.29 (H-21), δ_H 1.27 (H-28), δ_H 1.05 (H-19), and δ_H 0.96 (H-18)], two acetyl methyls [δ_H 2.01 and δ_H 1.88], three olefin methines [δ_H 5.79 (1H, br. d, *J* = 3.2 Hz, H-6); δ_H 7.06 (1H, d, *J* = 15.6 Hz, H-24); δ_H 6.76 (1H, d, *J* = 15.6 Hz, H-23)], including a double bond found to have a trans conformation from the coupling

constant ($J = 15.6$ Hz), and many methylenes and methines. The proton signals suggested that compound 1 is a pentacyclic triterpenoid with two acetyl groups (Supplementary Fig. 2b and Supplementary Table 3). The ^{13}C -NMR spectrum (150 MHz, CD_3OD , δ_{C}) presented 34 carbon signals including two acetyl groups (δ_{C} 171.8, 172.6, 22.0, 21.9). Also, the carbon signals of three ketones [δ_{C} 215.2 (C-3), δ_{C} 214.0 (C-11), and δ_{C} 204.6 (C-22)], one olefin quaternary [δ_{C} 142.2 (C-5)], three olefin methines [δ_{C} 153.0 (C-24), δ_{C} 121.9 (C-6), and δ_{C} 121.3 (C-23)], two oxygenated quaternaries [δ_{C} 81.0 (C-25) and δ_{C} 79.8 (C-20)], two oxygenated methines [δ_{C} 75.4 (C-2) and δ_{C} 73.0 (C-16)], four quaternaries [δ_{C} 52.0 (C-13), δ_{C} 51.7 (C-4), δ_{C} 49.9 (C-9), and δ_{C} 49.7 (C-14)], three methines [δ_{C} 56.3 (C-17), δ_{C} 43.9 (C-8), and δ_{C} 35.0 (C-10)], four methylenes [δ_{C} 49.9 (C-12), δ_{C} 44.5 (C-15), δ_{C} 37.2 (C-1), and δ_{C} 24.9 (C-7)], and eight methyls [δ_{C} 30.0 (C-28), δ_{C} 27.1 (C-27), δ_{C} 26.9 (C-26), δ_{C} 24.8 (C-21), δ_{C} 21.3 (C-29), δ_{C} 20.7 (C-19), δ_{C} 20.3 (C-18), and δ_{C} 19.4 (C-30)] were observed, indicating that compound 1 is a monoacetyl cucurbitacin B (Supplementary Fig. 3a and Supplementary Table 4). An oxygenated methine proton signal (H-16) was observed at 5.37 ppm due to downfield shifting, because of the esterification effect, which is usually observed around 4.30 ppm in cucurbitacin B⁶. This was confirmed from the cross peak between an oxygenated methine proton signal (δ_{H} 5.37, H-16) and an ester carbon signal of an acetyl group (δ_{C} 172.6) in the gHMBC spectrum (Supplementary Fig. 3b). By comparing the spectroscopic data with those in literature⁷, compound 1 was confirmed to be a 16-*O*-acetyl cucurbitacin B, a facacein, which was previously isolated from *Echinocystis esiacea*²³.

Elucidation of compound 2 (16-*O*-acetyl cucurbitacin D) structure by MS and NMR spectroscopy data analysis

The molecular formula of compound 2 was determined to be $\text{C}_{32}\text{H}_{46}\text{O}_8$ based on the negative ESI-MS m/z 603 $[\text{M}+\text{formic acid-H}]^-$ and HR ESI-MS m/z 603.3195 $[\text{M}+\text{formic acid-H}]^-$

(calculated for $C_{33}H_{47}O_{10}$ 603.3169) (Supplementary Fig. 4a). The molecular weight of compound 2 (558 amu) was 42 amu less than compound 1 (600 amu), indicating that compound 2 had one acetyl group less than compound 1. The 1H -NMR and ^{13}C -NMR spectra of compound 2 were very similar to those of compound 1, except for a shortage of signals arising from one acetyl moiety (Supplementary Figs. 4b and 5a). NMR spectroscopy data were similar to those of a cucurbitacin D, except for additional signals from one acetyl group (δ_H 1.83, 3H, s; δ_C 172.3, 21.2). Attachment of the acetyl group at C-16 was confirmed by a downfield shift of the oxygenated methine proton signal (H-16) to δ_H 5.30, which usually occurs at δ_H 4.3⁶. In the gHMBC spectrum (Supplementary Fig. 5b), an oxygenated methine proton signal δ_H 5.30 (H-16) showed cross-peaks with an ester carbon signal of an acetyl group (δ_C 172.3) and an oxygenated quaternary carbon signal δ_C 79.6 (C-20), indicating that the acetyl group was located at C-16. Taken together, compound 2 was identified as 16-*O*-acetyl cucurbitacin D, a novel compound.

Elucidation of compound 3 (16-*O*-acetyl cucurbitacin I) structure by MS and NMR spectroscopy data analysis

The molecular formula of compound 3 was determined to be $C_{32}H_{44}O_8$ based on the negative ESI-MS m/z 601 $[M+\text{formic acid}-H]^-$ and HR ESI-MS m/z 601.3026 $[M+\text{formic acid}-H]^-$ (calculated for $C_{33}H_{45}O_{10}$ 601.3012) (Supplementary Fig. 6a). The molecular weight of compound 3, 556 amu, was 2 amu less than compound 2 (558 amu) indicating that it possessed two hydrogens less than compound 2. The 1H -NMR and ^{13}C -NMR spectra of compound 3 were very similar to those of compound 2, except for the loss of signal due to an oxygenated methine and methylene, and an additional signals owing to an oxygenated olefin quaternary (δ_C 147.0, C-2) and an olefin methine (δ_H 5.74, 1H, d, $J=3.0$ Hz, H-1; δ_C 116.7, C-1) (Supplementary Figs. 6b and 7a). The NMR data were similar to those of a cucurbitacin I, except for the additional

signal of one acetyl group (δ_{H} 1.84, 3H, s; δ_{C} 172.3, 20.9). Due to a downfield shift of an oxygenated methine proton (δ_{H} 5.30; H-16), the position of acetyl was found to be C-16 of aglycone. In the gHMBC spectrum (Supplementary Fig. 7b), an oxygenated methine proton signal δ_{H} 5.32 (H-16) showed cross-peaks with an ester carbon signal of an acetyl group (δ_{C} 172.3) and an oxygenated quaternary carbon signal δ_{C} 79.6 (C-20), a quaternary carbon signal δ_{C} 49.7 (C-14), and a methine carbon signal δ_{C} 56.0 (C-17), indicating that the acetyl group was located at C-16. Taken together, compound 3 was identified to be a 16-*O*-acetyl cucurbitacin I, which was a new compound.

Elucidation of compound 4 (16-*O*-acetyl cucurbitacin E) structure by MS and NMR spectroscopy data analysis

The molecular formula of compound 4 was determined to be $\text{C}_{34}\text{H}_{46}\text{O}_9$ based on the negative ESI-MS m/z 643 $[\text{M}+\text{formic acid}-\text{H}]^-$ and HR ESI-MS m/z 643.3118 $[\text{M}+\text{formic acid}-\text{H}]^-$ (calculated for $\text{C}_{35}\text{H}_{47}\text{O}_{11}$ 643.3118) (Supplementary Fig. 8a). The molecular weight of compound 4, 598 amu, was 42 more than compound 3 (556 amu), indicating that compound 4 has one more acetyl group than compound 3. The ^1H -NMR and ^{13}C -NMR spectra of compound 4 were very similar to those of compound 3, except for the addition of an acetyl group signal (δ_{H} 1.90, 3H, s; δ_{C} 172.5, 21.3) (Supplementary Figs. 8b and 9a). From the oxygenated methine proton of H-16, there was a downfield shift according to the esterification effect, and the position of the acetyl group was revealed to be C-16. The gHMBC spectrum (Supplementary Fig. 9b), with an oxygenated methine proton signal δ_{H} 5.40 (H-16), was found to correlate with an acetyl carbonyl carbon signal (δ_{C} 172.5), an oxygenated quaternary carbon signal δ_{C} 79.8 (C-20), and an quaternary carbon signal δ_{C} 51.5 (C-13). Taken together, compound 4 was identified as a 16-*O*-acetyl curcurbitacin E, which was previously isolated from *Bacopa monnieri*²⁴.

Elucidation of compound 5 (2-*O*- β -D-glucopyranosyl 16-*O*-acetyl cucurbitacin E) structure by MS and NMR spectroscopy data analysis

The molecular formula of compound 5 was determined to be C₄₀H₅₆O₁₄ based on the negative ESI-MS *m/z* 805 [M+formic acid-H]⁻ and HR ESI-MS *m/z* 805.3693 [M+formic acid-H]⁻ (calculated for C₄₁H₅₇O₁₆ 805.3646) (Supplementary Fig. 10a). The molecular weight of compound 5, 760 amu, was 162 more than compound 4 (598 amu), suggesting that compound 5 has one hexose moiety more than compound 4. The ¹H-NMR and ¹³C-NMR spectra of compound 5 were very similar to those of compound 4, except for the additional hexose signals (Supplementary Figs. 10b and 11a). The sugar was determined to be a β -glucopyranose based on the chemical shift of the carbon signals due to an hemiacetal (δ_C 101.3, C-1'), four oxygenated methines (δ_C 75.3, C-2'; δ_C 77.7, C-3'; δ_C 70.7, C-4'; δ_C 78.3, C-5'), and an oxygenated methylene (δ_C 62.0, C-6') in the ¹³C-NMR spectrum, as well the coupling constant of the anomer proton signal ($J = 7.8$ Hz). In the HMBC spectrum, the anomer proton signal (δ_H 4.66, H-1') presented a cross peak with the oxygenated olefin quaternary carbon signal (δ_C 147.4, C-2), indicating that the sugar was linked to the hydroxyl group at C-2 (Supplementary Fig. 11b). Therefore, compound 5 was identified as a 2-*O*- β -D-glucopyranosyl 16-*O*-acetyl cucurbitacin E, which was previously isolated from *Gratiola officinalis*²⁵.

Semi RT-qPCR

To examine the expression of *ACTs* and *UGT* in unwounded and wounded watermelon leaves, samples were collected at certain times after wounding treatment and stored until total RNA extraction. For semi RT-qPCR analysis, total RNA was extracted from unwounded and wounded watermelon leaves using a RiboEx Total RNA Kit (GeneAll). RNA quality was determined using a Nanodrop ND-2000 spectrophotometer (Nanodrop Technologies), and only

high-quality RNA samples ($A_{260}/A_{230} > 2.0$ and $A_{260}/A_{280} > 1.8$) were used for subsequent experiments. cDNA synthesis was performed with 5 μg of total RNA using a SuperiorScript III Master Mix in accordance with the manufacturer's instructions (Enzynomics). cDNA (2 μL) fragments were used as templates for semi RT-qPCR using gene-specific forward and reverse primers (Supplementary Table 3). Semi RT-qPCR analysis was performed using a T100 thermal cycler (Bio-Rad) using a PCR Master mix solution (*i*-Taq) (INtRON). One stably expressed *TIP41* (*Cl**a016074*) gene was used as a reference gene (Supplementary Table 3). All semi RT-qPCR experiments were performed in two biological replicates (independently harvested samples). PCR products were analyzed using agarose gel electrophoresis to determine the relative abundance of transcripts.

References

- 1 Trapnell, C., Pachter, L. & Salzberg, S. L. TopHat: discovering splice junctions with RNA-Seq. *Bioinformatics* **25**, 1105-1111 (2009).
- 2 Trapnell, C. et al. Transcript assembly and quantification by RNA-Seq reveals unannotated transcripts and isoform switching during cell differentiation. *Nat Biotechnol* **28**, 511-515 (2010).
- 3 Trapnell, C. et al. Differential gene and transcript expression analysis of RNA-seq experiments with TopHat and Cufflinks. *Nat Protoc* **7**, 562-578 (2012).
- 4 Benjamini, Y. & Hochberg, Y. Controlling the False Discovery Rate - a Practical and Powerful Approach to Multiple Testing. *J R Stat Soc B* **57**, 289-300 (1995).
- 5 Fisher, R. A. On the Interpretation of χ^2 from Contingency Tables, and the Calculation of P. . *Journal of the Royal Statistical Society* **85**, 87-94 (1922).
- 6 Ayyad, S. E., Abdel-Lateff, A., Basaif, S. A. & Shier, T. Cucurbitacins-type triterpene with potent activity on mouse embryonic fibroblast from Cucumis prophetarum, cucurbitaceae. *Pharmacognosy Res* **3**, 189-193 (2011).
- 7 Ryu, J. S. & Lloyd, D. Cell Cytotoxicity of Sodium-Nitrite, Sodium-Nitroprusside and Roussins Black Salt against *Trichomonas-Vaginalis*. *Fems Microbiol Lett* **130**, 183-187 (1995).